



Delft University of Technology

Modelling the effect of plastic sheet curing on early age temperature development in concrete pavement

Ren, Dongya; Houben, Lambert

DOI

[10.1080/10298436.2018.1502431](https://doi.org/10.1080/10298436.2018.1502431)

Publication date

2018

Document Version

Accepted author manuscript

Published in

International Journal of Pavement Engineering

Citation (APA)

Ren, D., & Houben, L. (2018). Modelling the effect of plastic sheet curing on early age temperature development in concrete pavement. *International Journal of Pavement Engineering*, 21 (2020)(5), 559-570. <https://doi.org/10.1080/10298436.2018.1502431>

Important note

To cite this publication, please use the final published version (if applicable). Please check the document version above.

Copyright

Other than for strictly personal use, it is not permitted to download, forward or distribute the text or part of it, without the consent of the author(s) and/or copyright holder(s), unless the work is under an open content license such as Creative Commons.

Takedown policy

Please contact us and provide details if you believe this document breaches copyrights. We will remove access to the work immediately and investigate your claim.

Modelling the Effect of Plastic Sheet Curing on Early Age Temperature Development in Concrete Pavement

Prediction of the temperature development at early age is a good starting point to assess the development of the restrained thermal stress and thermal cracking in rigid pavements. This paper presents a numerical early age concrete pavement temperature prediction model. It enables to evaluate the effect of various paving conditions, such as paving time, curing method, air temperature, wind speed, and the concrete placement temperature, on the early age concrete pavement performance. A critical review of current heat flux models at the pavement surface covered with a plastic sheet is presented. An extension of existing models to quantify the effect of the plastic sheet curing method is introduced, based on the energy balance method. The numerical implementation procedure for the proposed temperature prediction model is solved by the finite difference method. The temperature prediction model was verified with field measured data of two test sections. The predicted temperature shows a satisfying match with field measured data. Lastly, the effect of plastic sheet curing and its duration on the development of the pavement temperature was analysed by the proposed theoretical model.

Keywords: temperature prediction; plastic sheet curing; early age; concrete pavement

INTRODUCTION

Fluctuations in temperature produce expansion and contraction in a concrete pavement, and when they are restrained, they lead to the development of stresses and possibly cracking, which may significantly affect the pavement's early age and long-term performance (Suh et al. 1992; Schindler et al. 2002). Several numerical models are available for evaluating the temperature and/or moisture distribution in concrete pavements, such as the well-known Enhanced Integrated Climatic Model (Dempsey et al. 1986), High performance concrete paving (Schindler et al. 2002), Temperature and Moisture Analysis for Curing Concrete (Yang 1996; Ye 2007). However, those models are not used in the correct way or that the models are not capable to accurately predict

the concrete temperature under curing conditions. The liquid curing compound, which is the most common curing method for concrete pavement construction, is used to protect the pavement concrete against drying out. For certain applications, the polyethylene sheeting together with the curing compound is commonly used in the concrete pavement construction practice. Polyethylene sheeting is very beneficial in retaining moisture of hardening concrete and thus minimizes the drying shrinkage. Polyethylene sheeting also acts as a thermal insulator as the use of insulation materials reduces the heat flux at the pavement surface. However, it can be detrimental if used improperly. It may result in too high concrete temperature in the summer construction conditions that thus cause damages following the concrete placement. For instance, the color of polyethylene sheeting is considered as the most critical variable that significantly increases the maximum concrete temperature and zero-stress temperature in a concrete pavement (Schindler et al. 2002). Besides, Figure 1 shows the measured concrete temperature at the top of the slab with and without the polyethylene sheet cover for a Continuously Reinforced Concrete Pavement (CRCP) section placed in July in Texas, United States. The difference between the maximum concrete temperatures at the 2nd day after paving is as high as 14°C at the top of the slab.

This paper describes in detail the development of an early age concrete pavement temperature prediction model that enables to simulate the use of blended slag cement and the plastic sheet curing method. This proposed model is then verified with field-measured data of two projects in Belgium.

EXISTING HEAT FLUX MODELS FOR PAVEMENT SURFACE WITH PLASTIC SHEET

An overall heat transfer coefficient proposed by McAdams (1954) to evaluate the convective heat transfer coefficients due to the presence of different insulation materials

is adopted in both MEPDG and HIPERPAV II (Ruiz et al. 2006):

$$h_0 = \left(\frac{1}{h_{conv}} + \frac{d_1}{k_1} + \frac{d_2}{k_2} + \dots + \frac{d_n}{k_n} \right)^{-1} \quad (1)$$

Where,

h_0 = the overall heat convection coefficient, [W/m²/°C];

d_1, d_2, \dots, d_n = thickness of n successive insulation layers, [m];

k_1, k_2, \dots, k_n = thermal conductivity of n successive insulation layers, [W/m/°C].

CIMS (1988), computer interactive maturity system, included some regression equations for the convective heat transfer coefficients to represent the heat loss by various insulation methods according to experiments results. These equations were derived by a best-fit curve in terms of wind velocity by using the least squares method, and those equations were implemented in the program CIMS. In case of the curing method by polyethylene sheeting, the following regression equation is proposed (adapted for the SI units):

$$h_{conv,ps,CIMS} = -0.0040v_{wind}^2 + 0.5156v_{wind} + 5.1461 \quad (2)$$

Where, the range of v_{wind} is from 0 to 10 m/s.

The thermal characteristics of various insulation materials were well summarized by Schindler et al. (2002). Normally, a clear polyethylene sheeting with a thickness of 0.15 mm is used immediately after the concrete placement. The thermal conductivity of such a polyethylene sheeting is chosen as 0.043 W/m/°C according to ASHRAE 1993 Handbook. Figure 2 shows the calculated convective heat transfer coefficients for cases with and without the polyethylene sheeting curing method. The method by HIPERPAV significantly overestimates the convective heat transfer coefficient with polyethylene sheeting as compared to that by the regression equation in

CIMS. It indicates that the treatment of heat flux for a pavement cured with polyethylene sheeting through the principle of an overall heat transfer coefficient is inadequate, which thus leads to underestimation of the pavement temperature. This problem has been noticed by the program developers of HIPERPAV when they verified the HIPERPAV model with temperature measurement data (Ruiz et al. 2006). It was found that using the real thickness of the plastic sheet would significantly underestimate the amount of heat retained by the pavement in case of the plastic sheet curing method. They interpreted that as follows: when a plastic sheet is used, it is not in full contact with the slab, and the air between concrete and sheet act as additional insulation. Finally, they recommended using an additional air layer thickness of 5 mm in addition to the plastic sheet in those cases where a plastic sheet is used. The air thermal conductivity at 20 °C is about 0.0257 W/m/K. As shown in Figure 2, the estimated heat convection coefficients by the calibrated model in HIPERPAV is close to the CIMS model that is in agreement with field measurements.

Besides, the calibrated overall heat convection model in HIPERPAV and the regression model in CIMS only account for the effect of a plastic sheet on the convective heat transfer, while its effects on the radiation are neglected. However, the radiation heat flux on the pavement surface alters as well when a plastic sheet is used, because the plastic sheet in general has different reflectance, transmittance, and absorbance for both shortwave radiation from the sun (0.2 to 1.2 μm) and the longwave radiation (2 to 50 μm) originating from the pavement surface and surrounding environment. For instance, it is well known that transparent polyethylene sheeting is widely used to increase the soil temperature in the agricultural field. The first part is the so-called greenhouse effect of the cover of the polyethylene sheeting through the reduction of heat losses by long wave radiation, especially when intensive cooling

occurs during the night. Another effect of polyethylene sheeting is the reduction of the evaporation, and thereby the reduction of the heat fluxes through the pavement surface. Thus, in case a plastic sheet is applied, a more fundamental heat transfer model initially proposed by Mahrer (1979) is adopted in the present study and it is briefly described as follows.

THEORETICAL HEAT FLUX MODEL FOR PAVEMENT SURFACE CONSIDERING PLASTIC SHEET

Mahrer (1979); Mahrer (1980); Mahrer et al. (1984); Ham and Kluitenberg (1994); Wu et al. (1996) have proposed one dimensional soil temperature models to predict the temperature of bare and mulched soil. In case of a pavement covered by polyethylene sheeting, the net heat flux at the pavement surface is determined as the sum of the net radiation flux, heat convection, and transmitted heat by conduction to the lower layers of the pavement structure.

The non-stationary heat conduction problem of the thermal behaviour of concrete during hardening can be described by the well-known Fourier equation (Narasimhan 1999), which relates the change of temperature over time to the change of temperature with depth considering the thermal properties.

$$\rho c \frac{\partial T}{\partial t} = \lambda \frac{\partial^2 T}{\partial x^2} + q(x, t) \quad (3)$$

Where, ρ , c , λ are the density, heat capacity and thermal conductivity of the pavement, respectively; T is pavement temperature as a function of time t and depth below the pavement surface x ; $q(x, t)$ is the rate of heat of cement hydration at time t under pavement depth x .

Heat balance equations for pavement surface

When a plastic sheet is applied, the net radiation fluxes Rn_p at the pavement surface consist of the net shortwave radiation (incoming shortwave solar radiation) and net longwave sky irradiance transmitted through the transparent plastic sheet, longwave radiation emitted from the plastic and pavement surface. Thus, the net radiation flux at the pavement surface with plastic sheet Rn_p is given by:

$$Rn_p = (1 - \alpha_p)\tau_s q_{sol}\rho^* + \varepsilon_p \tau_l \sigma T_{sky}^4 \rho_{ir}^* + \varepsilon_p \varepsilon_l \sigma T_{ps}^4 \rho_{ir}^* - (1 - \rho_l)\varepsilon_p \sigma T_s^4 \rho_{ir}^* \quad (4)$$

Where α_p is the short wave reflectivity of pavement surface; τ_s is short wave transmissivity of the plastic sheet; q_{sol} is the incoming instantaneous solar radiation; ε_p and ε_l are the emissivity of the pavement surface and plastic sheet, respectively; τ_l and ρ_l are transmissivity and reflectivity of the plastic sheet to the long wave radiation, respectively; T_s and T_{ps} are temperature of the pavement surface and the plastic sheet, respectively; T_{sky} is the estimated effective sky temperature of the surrounding environment; σ is Stefan-Boltzmann constant, $5.669 \times 10^{-8} \text{ W m}^{-2} \text{ K}^{-4}$.

As pavement is considered to be an opaque body, the short wave reflectivity of pavement surface $\alpha_p = 1 -$ the solar absorptivity of pavement surface. The solar absorptivity of concrete pavement is as function of surface color, concrete component and slab abrasion (Levinson and Akbari 2002; Ruiz et al 2006). McCullough and Rasmussen (1999) recommended typical values ranging from 0.5 to 0.6 for new and older concrete, respectively. In addition, the application of white curing compound reduces the solar absorptivity by 0.1 to 0.35. For this study, a solar absorptivity of 0.50 was chosen which is found most appropriate for concrete pavements cured with white curing compound according to several field temperature measurements (Schindler et al. 2002).

The effective sky temperature T_{sky} is the temperature of the surrounding environment, and is not equal to the ambient air temperature, and it is influenced by the dew point, water vapour pressure, sky cloud cover, etc. A simplified model proposed by Walton (1983) to calculate the effective sky temperature based on the dew point temperature, ambient temperature and the cloud cover is chosen in this study because the required inputs for the calculation of the effective temperature are available from meteorological stations. Moreover, Walton's model to calculate the effective sky temperature has been successfully used in several pavement temperature prediction models (Walton 1983; Bentz 2000). The effective sky temperature model proposed by Walton (1983) is expressed as:

$$T_{sky} = \varepsilon_{sky}^{0.25} \cdot T_a \quad (5)$$

$$\varepsilon_{sky} = 0.787 + 0.764 \cdot \ln \left(\frac{T_{dp} + 273}{273} \right) \cdot F_{cloud} \quad (6)$$

Where, T_a and T_{dp} are the ambient air temperature and dew point temperature, respectively; F_{cloud} is the cloud cover factor.

The variables ρ^* and ρ_{ir}^* in Equation (4) represent the multiple reflections of the shortwave and longwave radiation between the plastic sheet and pavement surface, respectively. For instance, considering the infinite transfer processes of short wave radiation under a polyethylene sheet as shown in Figure 3(a), the net solar short wave radiation $q_{sol,p}^*$ absorbed by the pavement surface with a polyethylene sheet is given by:

$$q_{sol,p}^* = \tau_s q_{sol} (1 - \alpha_p) + \tau_s q_{sol} \alpha_p \rho_s (1 - \alpha_p) + \tau_s q_{sol} \alpha_p^2 \rho_s^2 (1 - \alpha_p) + \tau_s q_{sol} \alpha_p^3 \rho_s^3 (1 - \alpha_p) + \dots \quad (7)$$

Where, ρ_s is the shortwave reflectivity of the plastic sheet, rearranging the terms at the right side of Equation (4) results in the following equation:

$$q_{sol,p}^* = \tau_s q_{sol} (1 - \alpha_p) (1 + \alpha_p \rho_s + \alpha_p^2 \rho_s^2 + \alpha_p^3 \rho_s^3 + \dots) \quad (8)$$

Based on Taylor series' approach, $(1 + \alpha_p \rho_s + \alpha_p^2 \rho_s^2 + \alpha_p^3 \rho_s^3 + \dots)$ equals $1/(1 - \alpha_p \rho_s)$, and for the sake of simplicity using the multiplier ρ^* in place of $1/(1 - \alpha_p \rho_s)$. Similarly, as shown in Figure 3(b), the variables ρ_{ir}^* accounting for the multiple reflections of longwave radiation can be obtained as follows:

$$\rho_{ir}^* = \frac{1}{1 - \rho_l(1 - \varepsilon_p)} \quad (9)$$

The air gap between the pavement surface and the polyethylene sheet is very thin, thus it is adequate to assume that the temperature of the trapped air is the same as the temperature of the polyethylene sheet T_{ps} . Moreover, the airflow through the wind does not affect the pavement surface covered by polyethylene sheeting, therefore, only the free heat convection is considered for the covered pavement surface. Finally, the heat convection $q_{conv,ps}$ at the pavement surface covered by a polyethylene sheet is calculated by:

$$q_{conv,ps} = h_{conv,pl}(T_{ps} - T_s) \quad (10)$$

Where, the convective heat transfer coefficient between the upper plastic sheet surface and the atmosphere is defined by the heat convection model in HIPERPAV II (Ruiz et al. 2006).

$$h_{conv} = 3.727 \cdot C \cdot (0.9 \cdot (T_s + T_a) + 32)^{-0.181} \cdot (T_s - T_a)^{0.266} \cdot \sqrt{1 + 2.857 \cdot v_{wind}} \quad (11)$$

Where, C is a constant correction factor depending on the heat flow condition, it is chosen as 1.79 when the pavement surface is warmer than the air, and 0.89 when the pavement surface is cooler than the air, v_{wind} is the wind speed near the pavement

surface. The convective heat transfer coefficient $h_{conv,ps}$ is determined through inputting a zero wind speed.

A polyethylene sheet normally does not transmit water. Therefore, the latent heat through evaporation in this study is taken as zero for the pavement surface covered with a polyethylene sheet. In the case of the hardening concrete, the heat generation rate of the cement hydration at the top surface layer $q_{c,s}$ should be also included. Therefore, the thermal balance equation for the covered pavement surface used in the present study is expressed by:

$$Rn_p + q_{conv,pl} + q_{c,s} - \lambda_c \left. \frac{\partial T}{\partial x} \right|_{surface} = \frac{\Delta x}{2} \cdot \rho_c \cdot c_c \cdot \frac{\partial T_s}{\partial t} \quad (12)$$

Where λ_c , ρ_c , c_c are the thermal conductivity, density, and heat capacity of the top concrete layer, respectively; Δx is the differential pavement thickness for the energy balance thickness of the pavement surface. In this study, the heat generation rate of the cement hydration at the top surface layer $q_{c,s}$ is determined by a concrete hydration model proposed by De Schutter (De Schutter and Taerwe 1985; Ren 2015). The above-mentioned thermal balance equation at the hardened pavement surface has been used successfully by several researchers (Gui et al. 2007; Han et al. 2011; Alavi et al. 2014). By combining Equation (4) and Equation (10), the heat balance Equation (12) for the covered pavement surface can be rewritten as:

$$(1 - \alpha_p) \tau_s q_{sol} \rho^* + \varepsilon_p \tau_l \sigma T_{sky}^4 \rho_{ir}^* + \varepsilon_p \varepsilon_l \sigma T_{ps}^4 \rho_{ir}^* - (1 - \rho_l) \varepsilon_p \sigma T_s^4 \rho_{ir}^* + h_{conv,pl}(T_{ps} - T_s) + q_{c,s} - \lambda_c \left. \frac{\partial T}{\partial x} \right|_{surface} = \frac{\Delta x}{2} \cdot \rho_c \cdot c_c \cdot \frac{\partial T_s}{\partial t} \quad (13)$$

Heat balance equations for plastic sheet surface

As shown in the Equations (13), the polyethylene sheet temperature T_{ps} must be known for

each time step. It can be obtained by the heat balance equation for the plastic sheet. Considering the rather thin thickness of a polyethylene sheet, the heat flux through conduction and evaporation is considered as zero, and the heat balance equation for the plastic sheet can thus be written as:

$$Rn_{ps} + h_{conv,ps}(T_s - T_{ps}) + h_{conv}(T_a - T_{ps}) = 0 \quad (14)$$

Where, Rn_{ps} is the net heat radiation for the plastic sheet; the subsequent two terms in Equation (14) represent the convective heat transfer between the lower plastic sheet surface and the underlying pavement surface, and between the upper plastic sheet surface and the atmosphere, respectively. Similar to the net radiation for the pavement surface, the net radiation Rn_{ps} for the plastic sheet is given by:

$$Rn_{ps} = q_{sol}[(1 - \rho_s) - \tau_s(1 - \alpha_p + \tau_s \alpha_p) \rho^*] + \sigma T_{sky}^4 [(1 - \rho_l) - \tau_l(\tau_l + \varepsilon_p(1 - \tau_l) \rho_{ir}^*) - \varepsilon_l \sigma T_{ps}^4 [2 - (1 - \varepsilon_p)(1 - \tau_l - \rho_l) \rho_{ir}^*] + \varepsilon_p \sigma T_s^4 [(1 - \tau_l - \rho_l) \rho_{ir}^*] \quad (15)$$

Where, ε_l is the emissivity of the plastic sheet that is equal to the longwave absorptivity of the plastic sheet, and is calculated from the corresponding longwave reflectivity and transmissivity of the plastic sheet ($\varepsilon_l = 1 - \tau_l - \rho_l$). Putting Equation (15) into Equation (14), the heat balance equation for the plastic sheet can be written as follows:

$$q_{sol}[(1 - \rho_s) - \tau_s(1 - \alpha_p + \tau_s \alpha_p) \rho^*] + \sigma T_{sky}^4 [(1 - \rho_l) - \tau_l(\tau_l + \varepsilon_p(1 - \tau_l) \rho_{ir}^*) - \varepsilon_l \sigma T_{ps}^4 [2 - (1 - \varepsilon_p)(1 - \tau_l - \rho_l) \rho_{ir}^*] + \varepsilon_p \sigma T_s^4 [(1 - \tau_l - \rho_l) \rho_{ir}^*] + h_{conv,ps}(T_s - T_{ps}) + h_{conv}(T_a - T_{ps}) = 0 \quad (16)$$

Lastly, the unique value of T_{ps} that simultaneously satisfies the heat balance Equation (16) for the plastic sheet is obtained by solving this quartic equation using MATLAB.

Optical properties of plastic sheet

The optical properties of the polyethylene sheet have been recognised as its primary parameters affecting the soil temperature (Mahrer 1979; Ham et al. 1993; Ham and Kluitenberg 1994). However, no European standard is currently available for selecting the type of polyethylene sheeting for concrete curing. Currently, ASTM C171 (2007) is the only available standard that covers sheet materials for curing concrete. Two types of polyethylene films, clear and white opaque, are included in ASTM C171. However, ASTM C171 only specifies that the minimum thickness of the used polyethylene films shall be not less than 0.10 mm and the daylight reflectance of the white opaque polyethylene sheet shall be at least 70%, and no more requirements are listed. The low-density clear polyethylene sheeting is commonly used for the initial curing of a concrete pavement in Belgium. Table 1 summarizes the reported optical properties for clear polyethylene sheets (Mahrer 1979; Sui and Zeng 1992; Ham and Kluitenberg 1994; Wu et al. 1996; Castro and Rey 2011). The moderate values of the optical properties reported by Ham and Kluitenberg (1994) are used in the present study: the transmissivity and reflectivity of shortwave radiation are 0.84 and 0.11, respectively, and the transmissivity and the reflectivity of longwave radiation are 0.78 and 0.17, respectively. According to the heat transfer theory, the emissivity of a body to the radiation of certain wavelength is equal to the relevant absorptivity, and the sum of the transmissivity, the reflectivity, and the emissivity equals a unity.

Figure 4 shows the calculated convective heat transfer at the pavement surface for the motorway E17 in Belgium by the new model considering the optical properties of the polyethylene sheet (Ren 2015). It clearly indicates that the polyethylene sheet reduce the convective heat flux significantly at the pavement surface. It is also observed that the convective heat flux is not sensitive to the wind speed when the pavement is covered by the plastic sheet curing.

MODEL VERIFICATION

Pavement temperature profiles in the early age are calculated by the finite difference method (Ren 2014 and 2015). The heat-diffusion problem of the hardening concrete is solved by an explicit finite difference method and the numerical prediction algorithm is implemented by MATLAB. Field measured temperature data of the CRCP pavement slab on the motorway E17 near Ghent (Belgium) in August 2011, and on the motorway E313 near Herentals (also in Belgium) in September 2012 are used to verify the proposed temperature prediction model (Ren 2012). Thermocouples were installed along various depth of the pavement slab and the temperatures are recorded at half hour intervals over a 72 hours period. The pavement structures of both worksites are designed under the current CRCP standard design concept in Belgium. The pavement structure consists of a 250 mm CRCP slab laid upon a 50 mm bituminous interlayer, a 150 mm roller compacted concrete base or lean concrete base, a sand subbase and the subgrade. However, it should be mentioned that the CRCP slab of E313 consists of two-lift construction, with a 50 mm top layer and 200 mm bottom layer constructed wet by wet. The depth of the simulation model is selected as 6.0 m and at that depth a constant ground temperature of 11.0°C, the approximation of the annual average air temperature in Belgium, is used. The computational domain is discretized in depth by 48 elements, with 10 elements for the pavement slab, 2 elements for the asphalt interlayer, 6 elements for the cement-stabilized base, 6 elements for the sand subbase, and 24 elements for the subgrade. The thickness and thermal parameters, tabulated in Table 2, of the pavement slab and the underlying layers are obtained from literatures (Thompson et al. 1987; Schindler et al. 2002). The time increment for each step is 180 seconds to ensure the convergence of the explicit numerical integration scheme considered in this approach.

The concrete mixture compositions, construction conditions, and hydration parameters for both case studies are listed in Table 3. The cement adopted in both cases is blast furnace slag cement, CEM III/A 42.5 N/LA, produced by Holcim. It contains 36% to 65% granulated blast furnace slag, with 410 m²/kg Blaine surface. Climatic input parameters are obtained from the nearest weather stations as shown in Figure 5. The ambient environmental conditions at any specific time are calculated by cubic spline interpolation of the values from the weather station records.

The required concrete hydration parameters of the De Schutter hydration model for both projects are obtained from the measured values through isothermal calorimetry conduction tests on paste samples. Due to space limitations, for more details about the proposed temperature model and the corresponding input parameters, reference is made to (Ren 2015).

RESULTS AND ANALYSIS

The estimated hourly concrete temperatures at various depths for both E313 and E17 are illustrated in Figure 6. The calculated results for both cases are quite close to the observed values. Moreover, the patterns of the estimated concrete temperatures at various depths are also similar to that of the corresponding observed temperatures. As shown in the Figure 6, the highest concrete temperature occurs during the first 24 hours after the concrete placement, which is due to the combination of external effects such as air temperature and internal effects of the generated hydration heat during the concrete curing process. The errors between estimated and observed temperature in the first 72 hours after concrete placement for both cases are summarized in Table 4. The deviations of the estimated and observed values are mostly within the ± 3.0 °C, and the largest deviations mainly occur at the first daytime when the internal heat of hydration generation rate is the highest.

The error analyses for the first 72 hours after concrete placement for both E17 and E313 are summarized in Table 4. The relative lower value of the Absolute Mean Error (AME) and the Root Mean Square Error (RMSE) indicates a reasonable fit between the observed and estimated temperatures for every location. Within each project, higher values of AME and RMSE are observed for the upper part of the pavement slab. The observed negative values of the Sum of Residuals (RES) in the project E17 as compared to $|\text{RES}|$ for all locations suggest that the proposed model consistently underestimates the actual temperature value. The predicted temperature at various depths shows much smaller discrepancies between the measurement data in the project E313. The correlation coefficients R^2 for all the locations for both cases are above 0.915 as shown in Figure 7, suggesting a very accurate fit, based on the overall first 72 hour data.

EFFECT OF PLASTIC SHEET COVER

To investigate the effect of the cover with the polyethylene sheet on the development of the concrete temperature and stress, two simulations have been conducted for various duration of the plastic sheet cover in summer condition, as shown in Figure 8 and Figure 9. The simulated examples include a morning placement (8 am) and an afternoon placement (4 pm). The other variables are sunny day, wind speed 3.5 m/s, the concrete placement temperature chosen equal to the air temperature at placement. The optical properties of the polyethylene sheet that is commonly used in Belgium concrete pavement practice are summarized in Table 3. Besides, the early age thermal stress development for CRCP in these two conditions are evaluated by a theoretical model proposed by Ren (2015), including a relaxation model for young concrete based on the degree of hydration and a step by step increment method used to calculate the stress history of hardening concrete. Due to space limitations, for more details about the proposed early age thermal stress development model for CRCP, reference is made to (Ren 2015).

Figure 8 shows the effect of the plastic sheet cover duration on the development of the slab temperature for the morning placement and afternoon placement in summer, respectively. The continuous grey line represents the air temperature. Almost without exception, the application of a plastic sheet cover significantly increases the concrete temperature in summer construction. In the morning paving example, the peak concrete temperature at the top of the slab (25 mm below the surface) increases from 37.6°C without plastic sheet cover to 45.3°C when the pavement is covered by a plastic sheet during 12 hours. The peak temperature further increases when the plastic sheet is applied longer and the peak temperature can even occur at the second day after placement. It is observed that a considerable large positive temperature difference between the surface and bottom of the pavement slab, larger than 10°C, develops at final set, which indicates a larger negative built-in temperature gradient. Another interesting finding is the rapid temperature drop when the plastic sheet is removed before the first night. Together with the corresponding low tensile strength present at that moment, it leads to the primary crack initiating during the first night. It may cause unwanted random cracks before the saw cuts are implemented. In case of afternoon placement on the summer day, the peak temperature at the top of the slab occurs at the second day following the concrete paving regardless of the plastic sheet cover duration. The peak temperature and the zero-stress temperature are slightly lower for the afternoon paved sections as compared to the section placed in the morning. Lastly, field survey shows that no cracks do occur during the first night when the concrete is placed in the afternoon or evening.

Figure 9 illustrates the effects of the plastic sheet cover duration on the development of the slab temperature and thermal stress for the morning placement and afternoon placement in autumn construction, respectively. It is clearly shown that the application of the plastic sheet curing method does not increase the zero-stress temperature considerably.

A much more uniform temperature distribution is also observed at the final set of concrete for the autumn construction cured by a plastic sheet.

If the plastic sheet curing method has to be used in sunny summer condition, due to the requirement of exposed aggregate surface treatment, one possible solution to avoid increasing the zero-stress temperature considerably is to select the adequate type of polyethylene sheeting. The optical properties of the polyethylene sheeting dominate the heat flux at the pavement surface thereby influencing the pavement temperature development in the early age. The type of polyethylene sheeting to be chosen depends on the concrete curing temperature. For instance, reflective sheeting should be used when curing temperatures exceed 30°C (ASTM C171 2007). On the contrary, dark coloured sheeting is recommended in cold season construction to help increasing the curing temperature.

CONCLUSIONS

This paper describes the processes of developing a theoretical heat flux model for concrete pavements with plastic sheet curing. A critical review of current heat flux models at the pavement surface with plastic sheet is presented. The method by HIPERPAV significantly overestimates the convective heat transfer coefficient with polyethylene sheeting which thus leads to underestimation of the pavement temperature. Besides, the calibrated overall heat convection model in HIPERPAV and the regression model in CIMS only account for the effect of a plastic sheet on the convective heat transfer, while its effects on the radiation are neglected.

An extension of existing models to quantify the effect of the plastic sheet curing method is introduced, based on the energy balance method. A simple numerical calculation using the finite differential method is presented. After that, the proposed temperature model is verified with field measurements on two concrete pavements in Belgium. The predicted

temperature shows a satisfying match with the data measured in the field.

Polyethylene sheet curing is very beneficial in capturing moisture of fresh concrete that minimizes the plastic shrinkage damage and reduces the drying shrinkage as well.

However, the polyethylene sheet curing method can be detrimental if used improperly. It could result in too high concrete temperatures in summer construction conditions that thus might cause damages following placement. If the plastic sheet curing method has to be used in sunny summer condition, due to the requirement of exposed aggregate surface treatment, one possible solution to avoid increasing the zero-stress temperature considerably is to select the adequate type of polyethylene sheeting. The proposed model enables to theoretically simulate the effects of a plastic sheet on the development of the concrete temperature and thermal stress.

REFERENCES

- Alavi, M., Pouranian, M., and Hajj, E. (2014). Prediction of Asphalt Pavement Temperature Profile with Finite Control Volume Method. *Transportation Research Record: Journal of the Transportation Research Board*, 2456, 96-106.
- ASTM C171 (2007). *Standard Specification for Sheet Materials for Curing Concrete*, ASTM International.
- De Castro, C. A., & Rey, O. P. (2011). Numerical study on transient heat transfer under soil with plastic mulch in agriculture applications using a nonlinear finite element model. *arXiv preprint arXiv:1110.1690*
- De Schutter, G., and Taerwe, L. (1995). "General hydration model for Portland cement and blast furnace slag cement." *Cement and Concrete Research*, 25(3), 593-604.
- Dempsey, B. J., Herlach, W. A., and Patel, A. J. (1986). "Climatic-Material-Structural Pavement Analysis Program." *Transportation Research Record: Journal of the Transportation Research Board*, 1095, 111-123.
- Digital Site Systems Inc (1988). "Computer interactive maturity system operating system." Pittsburgh.

- Gui, J., Phelan, P. E., Kaloush, K. E., and Golden, J. S. (2007). "Impact of pavement thermophysical properties on surface temperatures." *Journal of Materials in Civil Engineering*, 19(8), 683-690.
- Ham, J. M., Kluitenberg, G., and Lamont, W. (1993). "Optical properties of plastic mulches affect the field temperature regime." *Journal of the American Society for Horticultural Science*, 118(2), 188-193.
- Ham, J. M., and Kluitenberg, G. J. (1994). "Modeling the effect of mulch optical properties and mulch-soil contact resistance on soil heating under plastic mulch culture." *Agricultural and forest meteorology*, 71(3), 403-424.
- Han, R., Jin, X., & Glover, C. J. (2011). Modeling pavement temperature for use in binder oxidation models and pavement performance prediction. *Journal of materials in civil engineering*, 23(4), 351-359.
- Handbook, A. S. H. R. A. E. (2001). *Fundamentals*. American Society of Heating, Refrigerating and Air Conditioning Engineers, Atlanta, 111.
- Levinson, R., and Akbari, H. (2002). "Effects of Composition and Exposure on the Solar Reflectance of Portland Cement Concrete." *Cement and Concrete Research*, 32(11), 1679-1698.
- Mahrer, Y. (1979). "Prediction of soil temperatures of a soil mulched with transparent polyethylene." *Journal of applied meteorology*, 18(10), 1263-1267.
- Mahrer, Y. (1980). "A numerical model for calculating the soil temperature regime under transparent polyethylene mulches." *Agricultural Meteorology*, 22(3), 227-234.
- Mahrer, Y., Naot, O., Rawitz, E., and Katan, J. (1984). "Temperature and moisture regimes in soils mulched with transparent polyethylene." *Soil Science Society of America Journal*, 48(2), 362-367.
- McAdams, W. H. (1954). *Heat transmission*, McGraw-Hill, New York.
- McCullough, B. F., and Rasmussen, R. O. (1999). "Fast-track paving: concrete temperature control and traffic opening criteria for bonded concrete overlays volume I, Final Report." FHWA, US Department of Transportation.
- Nam, J. H. (2005). "Early-Age Behavior of CRCP and its Implications for Long-Term Performance." Doctoral Qin, Y. H. (2011). "Numerical Study on the Curling and Warping of Hardened Rigid Pavement Slabs." Doctoral Dissertation, Michigan Technological University, Houghton, MI, US.

- Narasimhan, T. N. (1999). Fourier's Heat Conduction Equation: History, Influence, and Connections. *Reviews of Geophysics*, 37(1), 151-172.
- Ren Dongya, L.J.M. Houben (2014). An Early Age Concrete Pavement Temperature Prediction Model, 8th International DUT-Workshop on Research and Innovations for Design of Sustainable and Durable Concrete Pavements. Prague, Czech Republic.
- Ren Dongya (2015), Optimisation of the Crack Pattern in Continuously Reinforced Concrete Pavements. "Doctoral Dissertation", Delft University of Technology, the Netherlands.
- Ren Dongya, L.J.M. Houben and Luc Rens (2012). Monitoring Early-age Cracking of Continuously Reinforced Concrete Pavements on the E17 at Ghent (Belgium), 2nd International Conference on Sustainable Construction Materials: Design, Performance and Application, ASCE, Wuhan, P.R. China.
- Ruiz, J. M., Rasmussen, R. O., Chang, G. K., Dick, J. C., Nelson, P. K., Schindler, A. K., Turner, D. J., and Wilde, W. J. (2006). "Computer-Based Guidelines for Concrete Pavements, Volume III: Technical Appendices." FHWA-HRT-04-127, Federal Highway Administration, Washington D.C. US.
- Schindler, A. K., Dossey, T., and McCullough, B. F. (2002). "Temperature Control during Construction to Improve the Long Term Performance of Portland Cement Concrete Pavements." Center for Transportation Research, The University of Texas at Austin, Texas, US.
- Suh, Y. C., Hankins, K. D., and McCullough, B. F. (1992). "Early-Age Behavior of Continuously Reinforced Concrete Pavement and Calibration of the Failure Prediction Model in the CRCP-7 Program." Center for Transportation Research, Bureau of Engineering Research, University of Texas at Austin, Austin, TX.
- Sui, H.-J., and Zeng, D.-C. (1992). "A Numerical Model for Simulating the Temperature and Moisture Regimes of Soil under Various Mulches." *Agricultural and Forest Meteorology*, 61(3), 281-299.
- Thompson, M. R., Dempsey, B. J., Hill, H., and Vogel, J. (1987). "Characterizing Temperature Effects for Pavement Analysis and Design." *Transportation Research Record: Journal of the Transportation Research Board*(1121), 14-22.
- Wu, Y., Perry, K. B., and Ristaino, J. B. (1996). "Estimating temperature of mulched and bare soil from meteorological data." *Agricultural and Forest Meteorology*, 81(3-4), 299-323.

- Yang, S. (1996). "A Temperature Prediction Model in New Concrete Pavement and a New Test Method for Concrete Fracture Pavements." Doctoral Dissertation, Texas A&M University, College Station, TX, United States.
- Ye, D. (2007). "Early Age Concrete Temperature and Moisture Relative to Curing Effectiveness and Projected Effects on Selected Aspects of Slab Behavior." Doctoral Dissertation, Texas A&M University, College Station, TX, United States.

Table 1. Optical properties of clear polyethylene sheet.

Author	Short wave optical properties		Longwave optical properties	
	transmissivity	reflectivity	transmissivity	reflectivity
Mahrer, 1979	0.880	0.220	0.700	0.300
Sui et al. 1992	0.840	--	0.750	--
Ham et al. 1994	0.840	0.110	0.780	0.170
Wu et al. 1996	0.890	0.060	0.800	0.160
De Castro et al. 2011	0.733	0.265	0.600	0.398

Table 2. Summary of thermal parameters of concrete slab and underlying layers.

Parameter	Concrete slab	Asphalt interlayer	Cement treated base	Sub-base	Subgrade
Thickness (m)	0.25	0.05	0.30	0.60	4.80
Space increment (m)	0.025	0.025	0.05	0.10	0.20
Time increment (s)	180	180	180	180	180
Density (kg/m ³)	2350	2300	2350	1800	2000
Heat capacity (J/m ³ /°C)	1000	1050	1000	900	1200
Heat conductivity (W/m/°C)	3.0	1.4	2.5	2.4	1.5

Table 3. Summary of input parameters for both case studies in Belgium.

Parameter	E17 Ghent	E313 Herentals	
		Top layer	Bottom layer
Construction Conditions			
Construction day and time	22:00, 18/08/2011	00:00, 12/09/2012	23:30, 11/09/2012
Fresh concrete temperature	25.0°C	22.5°C	22.5°C
Curing method (plastic sheet)¹			
Plastic sheet placement time	22:00, 18/08/2011	00:00, 12/09/2012	--
Plastic sheet removal time	15:00, 19/08/2011	13:30, 12/09/2012	--
Polyethylene sheet type		Clear low density polyethylene	
Shortwave radiation transmissivity		0.84	
Shortwave radiation reflectivity		0.11	
Longwave radiation transmissivity		0.78	
Longwave radiation reflectivity		0.17	
Pavement surface emissivity		0.80	
Pavement surface absorptivity		0.50	

Table 4. Summary of the statistics of hourly estimated and observed temperatures for the first 72 hours after concrete placement.

Statistics	E17			E313			
	50 mm	100 mm	225 mm	75 mm	100 mm	175 mm	22 5mm
R^2	0.915	0.948	0.951	0.951	0.954	0.967	0.980
AME	1.31	1.16	0.90	0.77	0.77	0.56	0.51
$RMSE$	1.67	1.37	1.08	1.00	0.99	0.79	0.63
RES	-73.39	-63.15	-47.64	2.26	6.82	-11.83	-24.35
$ RES $	95.87	84.71	65.48	56.32	56.39	40.80	37.30

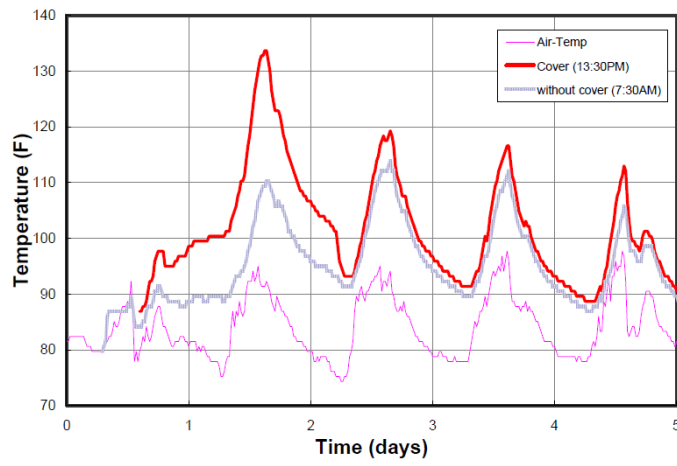


Figure 1. Measured concrete pavement surface temperature with and without plastic sheet cover, after Nam 2005.

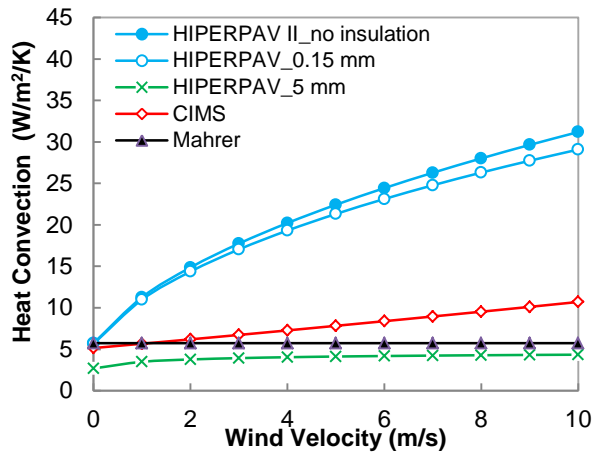


Figure 2. Comparison of heat convection models with plastic sheeting.

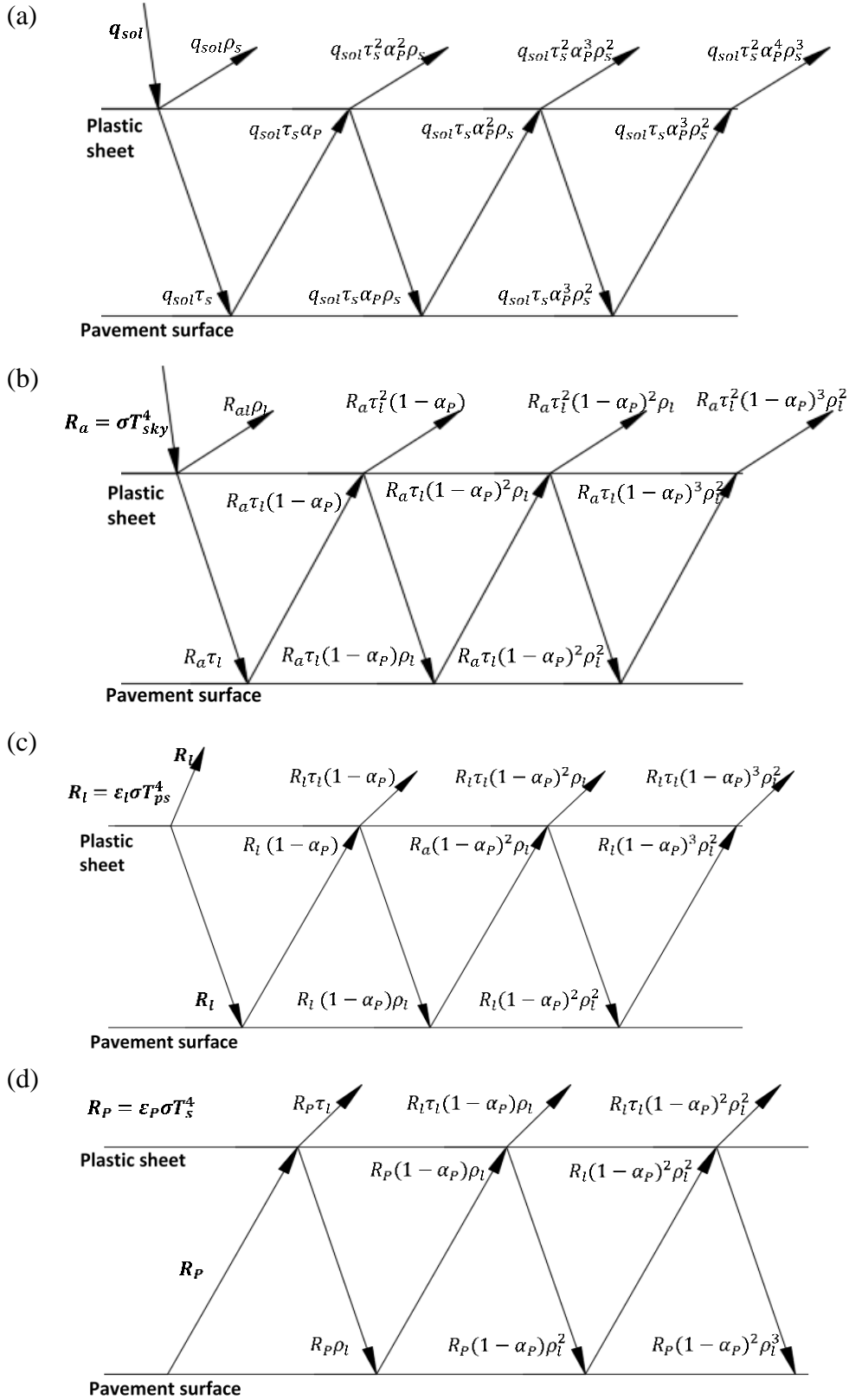


Figure 3. Schematic of multiple reflections of the short wave radiation (a), long wave sky irradiance (b), and long wave radiation from the plastic sheet (c) and pavement surface (d), respectively.

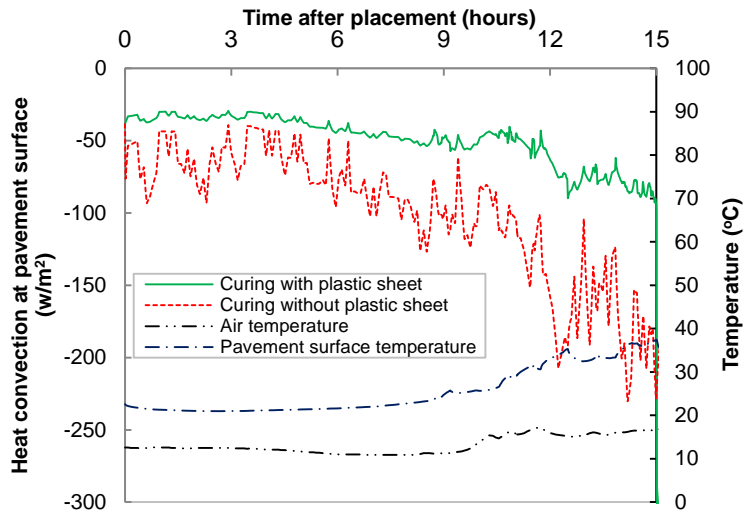


Figure 4. Comparison of net heat flux at the pavement surface with and without plastic sheet curing, E17, concrete placed at 22:00, August 18, 2011.

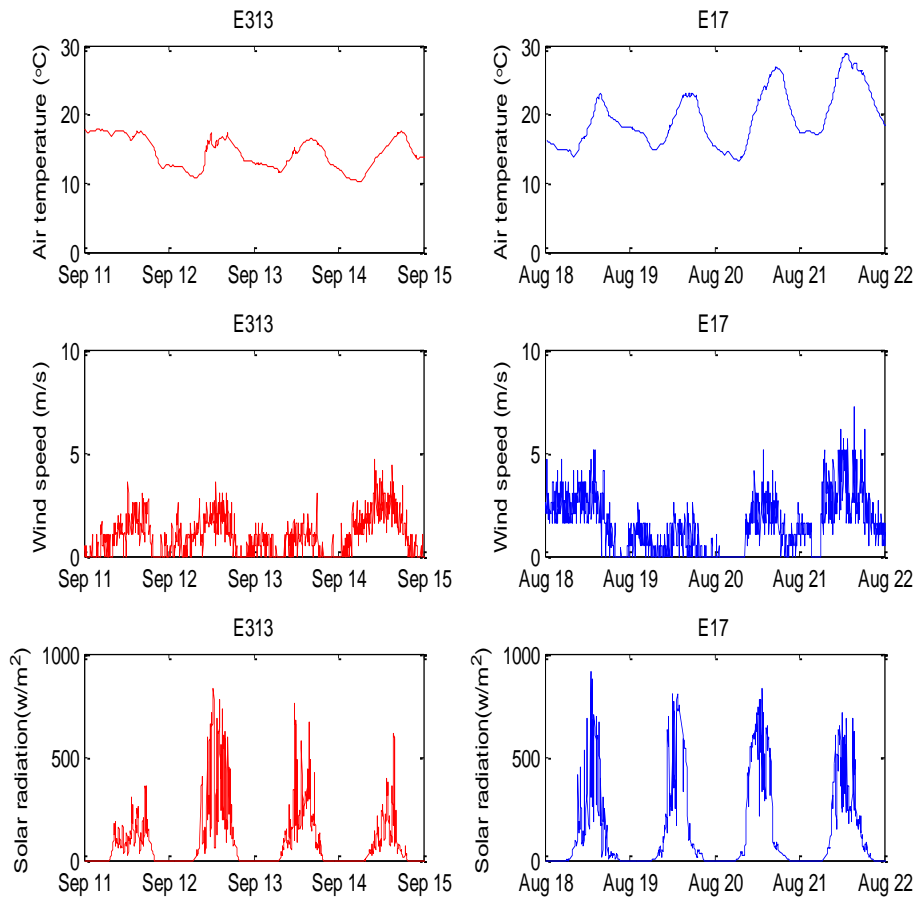
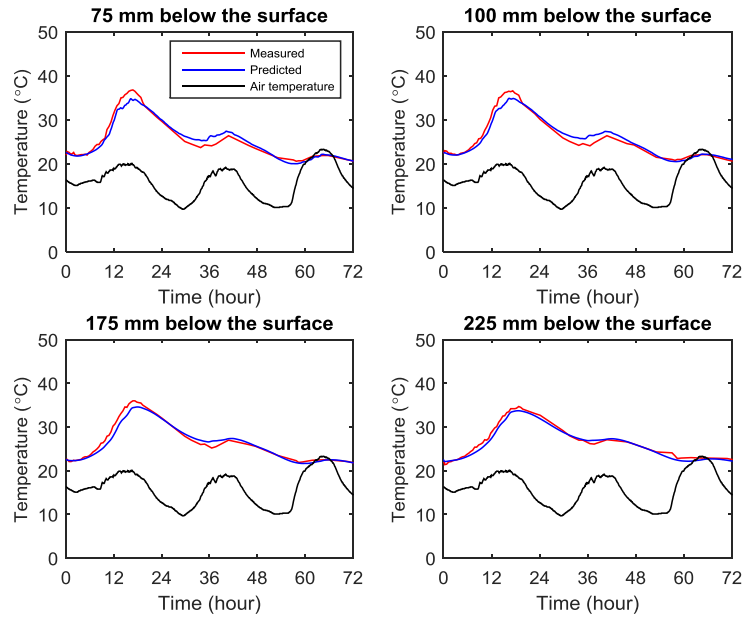
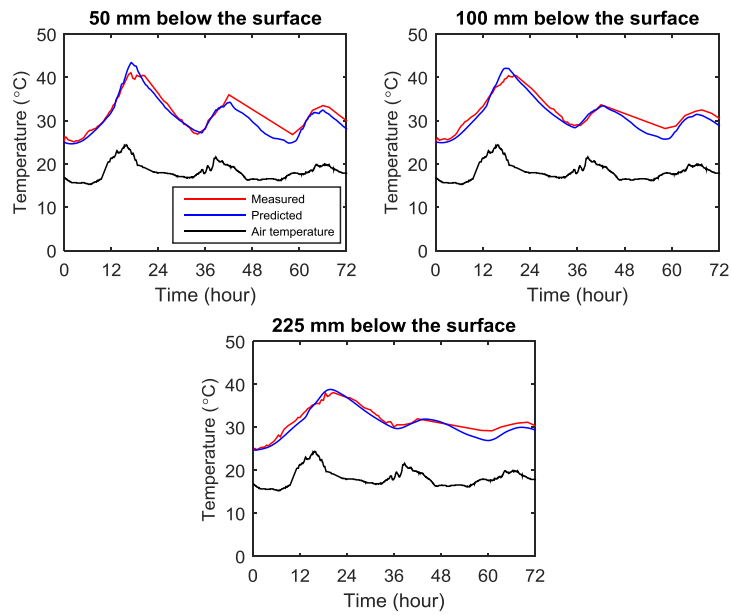


Figure 5. Air temperature, wind speed and solar radiation during the construction period for the work sites on E313 (September 2012) and E17 (August 2011), respectively.



(a)



(b)

Figure 6. Estimated and observed temperature at various depth of concrete slab during the first 72 hours after concrete placement (a) on E313, Herentals, September 12 to 15, 2012; (b) on E17, Ghent, August 19 to 22, 2011.

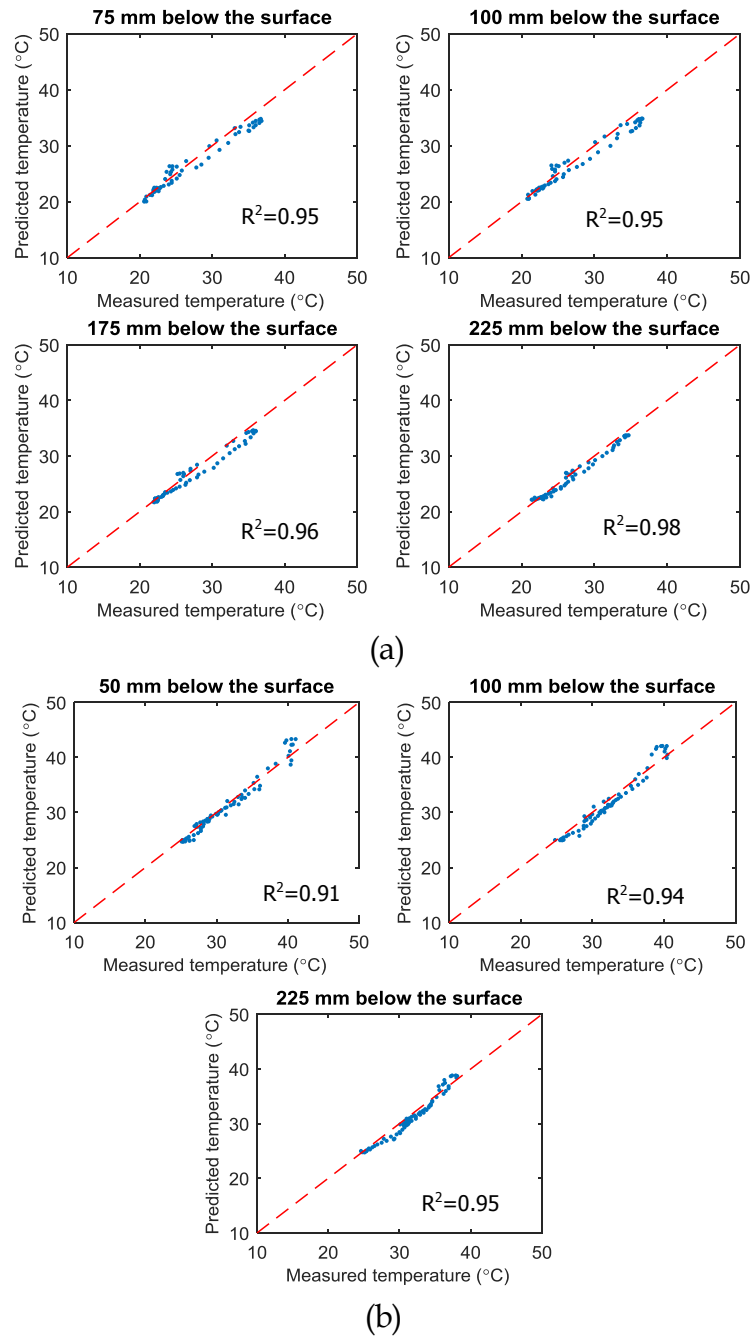
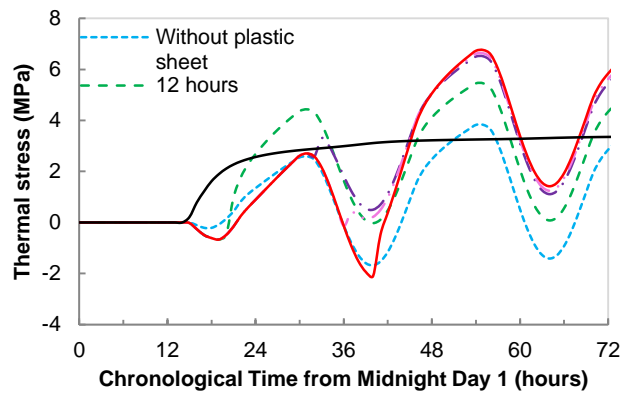
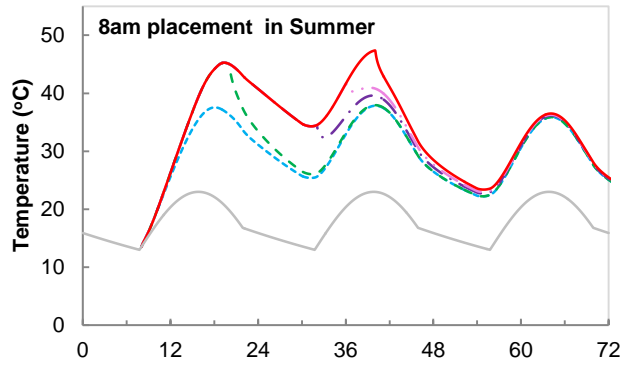
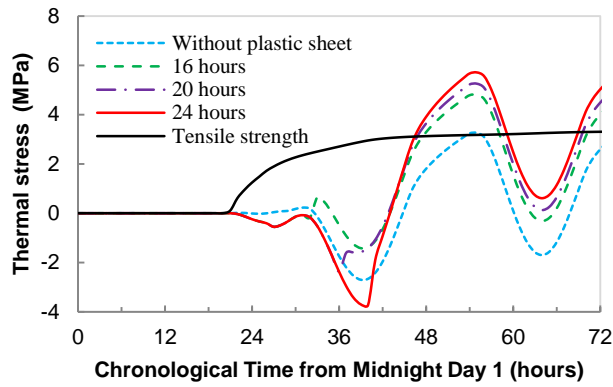
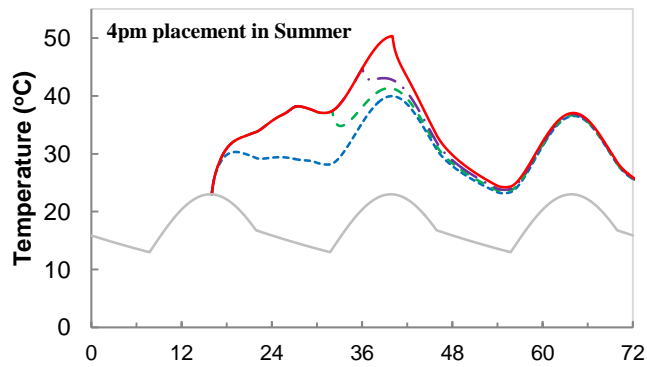


Figure 7. The linear correlation between the hourly estimated and observed temperature at various depth of concrete slab during the first 72 hours after concrete placement (a) on E313, Herentals, September 12 to 15, 2012; (b) on E17, Ghent, August 19 to 22, 2011.

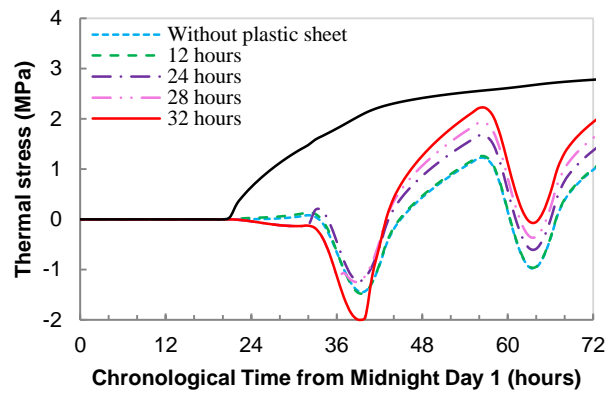
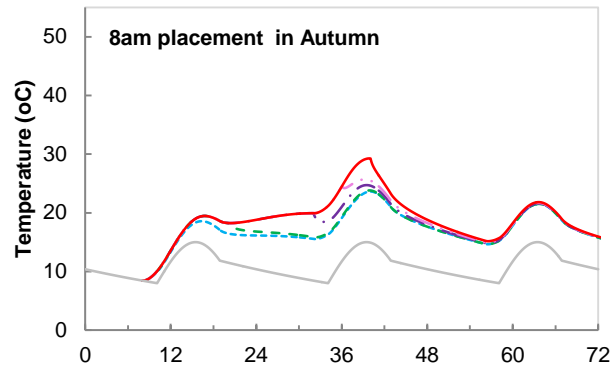


(a) 8 am

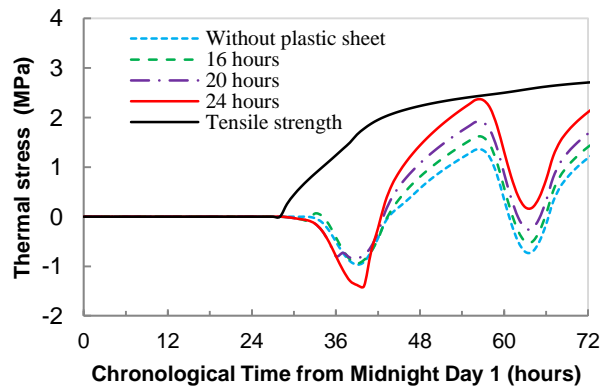
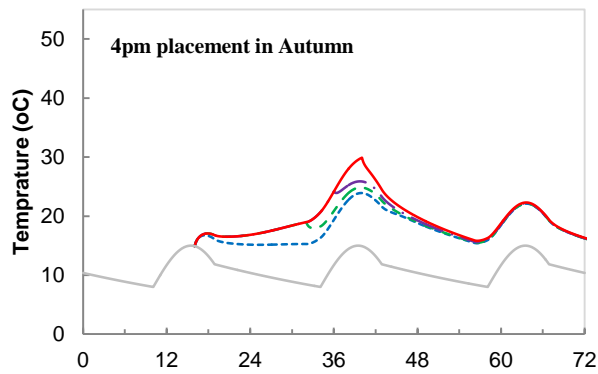


(b) 4 pm

Figure 8. Effect of duration of plastic sheet cover for summer construction. (a) 8 am; (b) 4 pm.



(a) 8 am



(b) 4 pm

Figure 9. Effect of duration of plastic sheet cover for autumn construction. (a) 8 am; (b) 4 pm.